

$B_s^0 - \bar{B}_s^0$ mixing within minimal flavor-violating two-Higgs-doublet models

Qin Chang^{a,c}, Pei-Fu Li^a and Xin-Qiang Li^{b,c*}

^aInstitute of Particle and Nuclear Physics, Henan Normal University, Henan 453007, P. R. China

^bInstitute of Particle Physics and Key Laboratory of Quark and Lepton Physics (MOE),
Central China Normal University, Wuhan, Hubei 430079, P. R. China

^cState Key Laboratory of Theoretical Physics, Institute of Theoretical Physics,
Chinese Academy of Sciences, P. R. China

Abstract

In the ‘‘Higgs basis’’ for a generic 2HDM, only one scalar doublet gets a nonzero vacuum expectation value and, under the criterion of minimal flavor violation, the other one is fixed to be either color-singlet or color-octet, which are named as the type-III and type-C models, respectively. In this paper, the charged-Higgs effects of these two models on $B_s^0 - \bar{B}_s^0$ mixing are studied. Firstly, we perform a complete one-loop computation of the electro-weak corrections to the amplitudes of $B_s^0 - \bar{B}_s^0$ mixing. Together with the up-to-date experimental measurements, a detailed phenomenological analysis is then performed in the cases of both real and complex Yukawa couplings of charged scalars to quarks. The spaces of model parameters allowed by the current experimental data on $B_s^0 - \bar{B}_s^0$ mixing are obtained and the differences between type-III and type-C models are investigated, which is helpful to distinguish between these two models.

PACS numbers: 13.25.Hw 12.60.Fr 14.80.Fd

*Corresponding author: xqli@itp.ac.cn

1 Introduction

Thanks to the successful running of the Large Hadron Collider (LHC), particle physics has entered a new era, which is featured by the discovery of a new boson with a mass close to 125 GeV [1, 2]. Its measured properties are so far in good agreement with those of the Standard Model (SM) Higgs [3–5], suggesting that the electro-weak symmetry breaking (EWSB) is probably realized via the Higgs mechanism implemented through a single scalar doublet. It should be noted, however, that the EWSB is not necessarily induced by just a single scalar. Interestingly, many new physics (NP) scenarios are equipped with an extended scalar sector. The search for additional scalars is one of the important programs of the LHC experiments.

One of the extensions of SM scalar sector is the so-called two-Higgs-doublet model (2HDM) [6], in which a second scalar doublet is added to the SM field content. To avoid the experimental constraints on flavor-changing neutral-current (FCNC) transitions, which are forbidden at tree level in the SM due to the GIM mechanism [7], two different hypotheses, natural flavor conservation (NFC) [8] and minimal flavor violation (MFV) [9], have been proposed ¹. In the NFC hypothesis, depending on the Z_2 charge assignments on the scalar doublets and fermions, there exist four types of 2HDM (type-I, II, X and Y) [11]. In the MFV hypothesis, to control the flavor-violating interactions, all the scalar Yukawa couplings are assumed to be composed of the SM ones Y^U and Y^D . In the “Higgs basis” [12], in which only one doublet gets a nonzero vacuum expectation value (VEV) and behaves as the SM one, the allowed $SU(3)_C \otimes SU(2)_L \otimes U(1)_Y$ representation of the second scalar doublet that couples to quarks via Yukawa interactions is fixed to be either $(1, 2)_{1/2}$ or $(8, 2)_{1/2}$ [13], which implies that the second scalar doublet can be either color-singlet or color-octet. For convenience, they are referred to as type-III and type-C models [14], respectively. Examples of the former include the aligned 2HDM (A2HDM) [15] and the four types of 2HDM reviewed in Ref. [11]. The scalar spectrum of the latter contains, besides a CP-even and color-singlet Higgs boson (the usual SM one), three color-octet particles, one CP-even, one CP-odd and one electrically charged [13].

Although the scalar-mediated flavor-violating interactions are protected by the MFV hypothesis, the type-III and type-C models still present very interesting phenomena in some

¹The NFC and MFV hypotheses are not the only alternatives to avoid constraints from FCNCs; models with controlled FCNCs have also been addressed in the literature and shown to be compatible with the data [10].

low-energy processes, especially due to the presence of a charged Higgs boson [13, 14, 16]. In this paper, we shall study the $B_s^0 - \bar{B}_s^0$ mixing within these two models and pursue possible differences between their effects. Since the charged Higgs contributes to the process at the same order as does the W boson in the SM, the NP effects might be significant.

It is known that the $B_s^0 - \bar{B}_s^0$ mixing, which is governed by a Schrödinger equation and induced by the $b \rightarrow s$ transition, plays an important role in accurate tests of the SM and indirect searches for NP. In terms of the off-diagonal elements of the mass and decay matrices, M_{12}^s and Γ_{12}^s , the mass and width differences between the two mass eigenstates $|B_H\rangle$ and $|B_L\rangle$ are defined, respectively, by

$$\Delta M_s \equiv M_H - M_L = 2|M_{12}^s|, \quad \Delta\Gamma_s \equiv \Gamma_L - \Gamma_H = 2|\Gamma_{12}^s| \cos \phi_s, \quad (1)$$

where $\phi_s \equiv \arg(-M_{12}^s/\Gamma_{12}^s)$ is the CP-violating phase. Such two observables have been measured precisely, with the averaged values given, respectively, by [17]

$$\Delta M_s^{exp.} = 17.757 \pm 0.021 \text{ ps}^{-1}, \quad \Delta\Gamma_s^{exp.} = 0.081 \pm 0.006 \text{ ps}^{-1}, \quad (2)$$

which are in good agreement with the recent SM predictions, $\Delta M_s^{SM} = (17.3 \pm 2.6) \text{ ps}^{-1}$ and $\Delta\Gamma_s^{SM} = (0.087 \pm 0.021) \text{ ps}^{-1}$ [18].

There are another two interesting observables related to $B_s^0 - \bar{B}_s^0$ mixing, the flavor-specific CP asymmetry a_{sl}^s and the CP-violating phase $\phi_s^{c\bar{c}s}$ ², which are defined, respectively, by

$$a_{sl}^s = \text{Im} \frac{\Gamma_{12}^s}{M_{12}^s} = \frac{\Delta M_s}{\Delta\Gamma_s} \tan \phi_s, \quad \phi_s^{c\bar{c}s} = \arg(M_{12}^s). \quad (3)$$

For $\phi_s^{c\bar{c}s}$, the SM prediction ~ -0.036 [18] agrees with the experimental data -0.015 ± 0.035 [17] within 1σ error bar. For a_{sl}^s , on the other hand, the measurement $(-0.75 \pm 0.41)\%$ [17] is significantly different from the SM estimation $\sim \mathcal{O}(10^{-5})$ [18], even though they are in agreement with each other at 1.5σ level due to the large experimental error bars. Under the constraints of the above four observables, the allowed NP spaces could possibly be strictly reduced. So, in this paper, we shall evaluate the effects of charged Higgs in type-III and type-C 2HDMs on $B_s^0 - \bar{B}_s^0$ mixing, and pursue possible differences between these two models.

²The phase $\phi_s^{c\bar{c}s}$ appears in tree-dominated $b \rightarrow c\bar{c}s$ B_s decays, such as $B_s \rightarrow J/\psi\phi$, and is generally different from ϕ_s unless the terms proportional to $V_{cb}V_{cs}^*V_{ub}V_{us}^*$ and $(V_{ub}V_{us}^*)^2$ in Γ_{12}^s are neglected [19].

Our paper is organized as follows. In Sec. 2, after a brief review of the 2HDMs under the MFV hypothesis, we perform a complete one-loop computation of the electro-weak corrections to the amplitudes of $B_s^0 - \bar{B}_s^0$ mixing within the two models. In Sec. 3, the numerical results and discussions are presented in detail. Finally, our conclusions are made in Sec. 4. Explicit expressions for the loop functions appearing in $B_s^0 - \bar{B}_s^0$ mixing are collected in the appendix.

2 Theoretical Framework

2.1 Brief review of the 2HDMs under the MFV hypothesis

Firstly, for convenience and consistence, we shall give a brief review of the 2HDMs under the MFV hypothesis. In the ‘‘Higgs basis’’, the Yukawa interactions of the two Higgs fields Φ_1 and Φ_2 with quarks are given by [13, 14]

$$-\mathcal{L}_Y = \bar{q}_L^0 \tilde{\Phi}_1 Y^U u_R^0 + \bar{q}_L^0 \Phi_1 Y^D d_R^0 + \bar{q}_L^0 \tilde{\Phi}_2^{(a)} T_R^{(a)} \bar{Y}^U u_R^0 + \bar{q}_L^0 \Phi_2^{(a)} T_R^{(a)} \bar{Y}^D d_R^0 + \text{h.c.}, \quad (4)$$

where q_L^0 , u_R^0 and d_R^0 are the quark fields in the interaction basis; $T_R^{(a)}$ is the $SU(3)_C$ generator and determines the color nature (color-singlet or color-octet) of the second scalar doublet; $Y^{U,D}$ and $\bar{Y}^{U,D}$ denote the Yukawa couplings and are generally complex 3×3 matrices in the quark flavor space. According to the MFV hypothesis, the transformation properties of the Yukawa coupling matrices $Y^{U,D}$ and $\bar{Y}^{U,D}$ under the quark flavor symmetry group $SU(3)_{Q_L} \otimes SU(3)_{U_R} \otimes SU(3)_{U_D}$ are required to be the same. This can be achieved by requiring $\bar{Y}^{U,D}$ to be composed of pairs of the matrices $Y^{U,D}$ [14]

$$\begin{aligned} \bar{Y}^U &= A_u^* (1 + \epsilon_u^* Y^U Y^{U\dagger} + \dots) Y^U, \\ \bar{Y}^D &= A_d (1 + \epsilon_d Y^U Y^{U\dagger} + \dots) Y^D, \end{aligned} \quad (5)$$

where the ellipses denote trivial terms involving higher power of $Y^U Y^{U\dagger}$ and powers of $Y^D Y^{D\dagger}$.

After applying the SM unitary transformations to rotate the fermionic fields from the interaction to the mass-eigenstate basis, one can finally obtain the Yukawa interactions of charged Higgs bosons with quarks in the mass-eigenstate basis [14, 16]

$$\mathcal{L}_{H^\pm} = \frac{g}{\sqrt{2}m_W} \sum_{i,j=1}^3 \bar{u}_i T_R^{(a)} (A_u^i m_{u_i} P_L - A_d^i m_{d_j} P_R) V_{ij} d_j H_{(a)}^\pm + \text{h.c.}, \quad (6)$$

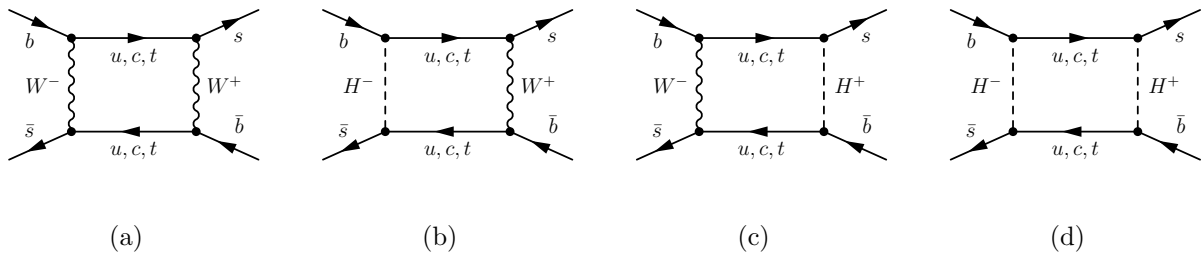


Figure 1: Box diagrams relevant to the $B_s^0 - \bar{B}_s^0$ mixing in the unitary gauge, both within the SM (the first one) and in the 2HDMs with MFV (the last three ones). We have also taken into account the crossed diagrams, which are related to the original ones by interchanging the external lines.

where g is the $SU(2)_L$ coupling constant, i, j the fermionic generation indices, and $m_{u,d}$ the quark masses; V denotes the Cabibbo–Kobayashi–Maskawa (CKM) matrix [20,21], and $P_{R,L} = \frac{1 \pm \gamma_5}{2}$ are the right- and left-handed chirality projectors. The couplings $A_{u,d}^i$ are generally family-dependent and read

$$A_{u,d}^i = A_{u,d} \left(1 + \epsilon_{u,d} \frac{m_t^2}{v^2} \delta_{i3} \right), \quad (7)$$

where $v = \langle \Phi_1^0 \rangle = 174$ GeV. Since only the couplings of charged Higgs bosons to the top quark are involved for $B_s^0 - \bar{B}_s^0$ mixing, we shall drop the family index in $A_{u,d}^i$ from now on.

Following the notation used in Ref. [14], we shall denote the model with the second scalar doublet being color-singlet and the one with the second scalar doublet color-octet as the type-III and the type-C model, respectively, both of which satisfy the principle of MFV. Their explicit contributions to the $B_s^0 - \bar{B}_s^0$ mixing will be presented in the next subsection.

2.2 $B_s^0 - \bar{B}_s^0$ mixing within the SM and the 2HDMs with MFV

Within the 2HDMs with MFV, the $B_s^0 - \bar{B}_s^0$ mixing occurs through the box diagrams shown in Figs. 1(b)-(d), which are obtained from the SM one (Fig. 1(a)) with the W^\pm propagator(s) replaced by the charged-Higgs H^\pm one(s). After calculating these one-loop box diagrams and applying the standard procedure of matching [22,23], one can obtain the 2HDM corrections to the $B_s^0 - \bar{B}_s^0$ mixing. Together with the SM contribution, the resulting effective weak Hamiltonian responsible for $B_s^0 - \bar{B}_s^0$ mixing can be written as

$$\mathcal{H}_{eff}^{full} = \frac{G_F^2}{16\pi^2} m_W^2 (V_{tb}V_{ts}^*)^2 [C^{VLL}(\mu)O^{VLL} + C^{SRR}(\mu)O^{SRR} + C^{TRR}(\mu)O^{TRR}] + \text{h.c.}, \quad (8)$$

where G_F is the Fermi coupling constant, and $C_i(\mu)$ the scale-dependent Wilson coefficients of the four-quark operators O_i , which are defined, respectively, as

$$\begin{aligned} O^{VLL} &= \bar{s}^\alpha \gamma_\mu (1 - \gamma_5) b^\alpha \bar{s}^\beta \gamma^\mu (1 - \gamma_5) b^\beta, \\ O^{SRR} &= \bar{s}^\alpha (1 + \gamma_5) b^\alpha \bar{s}^\beta (1 + \gamma_5) b^\beta, \\ O^{TRR} &= \bar{s}^\alpha \sigma_{\mu\nu} (1 + \gamma_5) b^\alpha \bar{s}^\beta \sigma^{\mu\nu} (1 + \gamma_5) b^\beta, \end{aligned} \quad (9)$$

with α, β being the color indices and $\sigma_{\mu\nu} = \frac{1}{2}[\gamma_\mu, \gamma_\nu]$. In addition, the hadronic matrix elements of the four-quark operators can be parameterized as [24]

$$\begin{aligned} \langle B_s^0 | O^{VLL} | \bar{B}_s^0 \rangle &= \frac{8}{3} m_{B_s}^2 f_{B_s}^2 B_1(\mu_b), \\ \langle B_s^0 | O^{SRR} | \bar{B}_s^0 \rangle &= -\frac{5}{3} \left(\frac{m_{B_s}}{\bar{m}_b(\mu_b) + \bar{m}_s(\mu_b)} \right)^2 m_{B_s}^2 f_{B_s}^2 B_2(\mu_b), \\ \langle B_s^0 | O^{TRR} | \bar{B}_s^0 \rangle &= \frac{4}{3} \left(\frac{m_{B_s}}{\bar{m}_b(\mu_b) + \bar{m}_s(\mu_b)} \right)^2 m_{B_s}^2 f_{B_s}^2 [-5B_2(\mu_b) + 2B_3(\mu_b)], \end{aligned} \quad (10)$$

where f_{B_s} is the B_s -meson decay constant, and $B_i(\mu_b)$ are the non-perturbative bag parameters calculated on the lattice at a characteristic scale $\mu_b \sim \mathcal{O}(m_b)$ [25].

The Wilson coefficients $C_i(\mu)$ in Eq. (8) consist of both the SM and 2HDM contributions and the results at the initial scale $\mu_W \sim \mathcal{O}(m_W, m_t, m_{H^\pm})$ can be written as

$$\begin{aligned} C^{VLL}(\mu_W) &= C_{SM}^{VLL}(\mu_W) + C_{2HDM}^{VLL}(\mu_W), \\ C^{SRR}(\mu_W) &= C_{SM}^{SRR}(\mu_W) + C_{2HDM}^{SRR}(\mu_W), \\ C^{TRR}(\mu_W) &= C_{SM}^{TRR}(\mu_W) + C_{2HDM}^{TRR}(\mu_W). \end{aligned} \quad (11)$$

Within the SM, the explicit expressions of the Wilson coefficients are computed from the box diagram shown in Fig. 1(a), accompanied by perturbative QCD corrections up to the desired order, details of which could be found, for example, in Refs. [22, 23, 26]. Including the next-to-leading order (NLO) QCD corrections, the SM contribution is given by [22, 23, 26]

$$C_{SM}^{VLL}(\mu_W) = S_0(x_t) + \frac{\alpha_s(\mu_W)}{4\pi} [S_1(x_t) + F(\mu_W)S_0(x_t) + B_t S_0(x_t)], \quad (12)$$

where $x_t = \frac{\bar{m}_t^2(\mu_W)}{m_W^2}$, and the leading order (LO) coefficient $S_0(x_t)$ is the known Inami-Lim function [27]. Generally, the SM also contributes to C^{SRR} and C^{TRR} and, in the absence of

QCD corrections, we get

$$C_{SM}^{SRR}(\mu_W) = \frac{x_b}{6} \left[\frac{x_t^2(5 - 22x_t + 5x_t^2)}{3(1 - x_t)^4} + \frac{x_t^2(1 - 3x_t - 3x_t^2 + x_t^3) \ln x_t}{(1 - x_t)^5} \right], \quad (13)$$

$$C_{SM}^{TRR}(\mu_W) = \frac{x_b}{6} \left[-\frac{5 - 15x_t + 8x_t^2 - 15x_t^3 + 5x_t^4}{3(1 - x_t)^4} + \frac{(1 - 5x_t + 9x_t^2 - x_t^3) \ln x_t}{(1 - x_t)^5} \right], \quad (14)$$

with $x_b = \frac{\bar{m}_b^2(\mu_W)}{m_W^2}$. It is obvious that both $C_{SM}^{SRR}(\mu_W)$ and $C_{SM}^{TRR}(\mu_W)$ are suppressed by the factor x_b and are, therefore, usually neglected in the literature [22].

The charged-Higgs contributions to the Wilson coefficients are computed from the last three box diagrams shown in Fig. 1, and depend on the two Yukawa coupling parameters A_u and A_d , as well as the charged-Higgs mass m_{H^\pm} [23, 29–32]. For the most general values of these parameters, especially when $A_d/A_u \simeq m_t/m_b$, each term in Eq. (6) can give a comparable contribution and should be, therefore, taken into account simultaneously. Explicitly, for the color-singlet charged-Higgs contributions (type-III model), we get

$$C_{III}^{VLL}(\mu_W) = A_u A_u^* f_1(x_t, x_h) + A_u^2 A_u^{*2} f_2(x_t, x_h), \quad (15)$$

$$C_{III}^{SRR}(\mu_W) = -x_b \left[A_u A_u^* f_3(x_t, x_h) + A_d A_u^* f_4(x_t, x_h) + A_d^2 A_u^{*2} f_5(x_t, x_h) \right. \\ \left. + A_u^2 A_u^{*2} f_6(x_t, x_h) + A_d A_u A_u^{*2} f_7(x_t, x_h) \right], \quad (16)$$

$$C_{III}^{TRR}(\mu_W) = 0, \quad (17)$$

where $x_h = m_{H^\pm}^2/m_W^2$, and the explicit expressions for $f_i(x_t, x_h)$ are collected in the appendix. For the color-octet charged-Higgs contributions (type-C model), on the other hand, we get

$$C_C^{VLL}(\mu_W) = \frac{1}{3} A_u A_u^* f_1(x_t, x_h) + \frac{11}{18} A_u^2 A_u^{*2} f_2(x_t, x_h), \quad (18)$$

$$C_C^{SRR}(\mu_W) = -x_b \left[-\frac{5}{12} A_u A_u^* f_3(x_t, x_h) - \frac{5}{12} A_d A_u^* f_4(x_t, x_h) - \frac{19}{72} A_d^2 A_u^{*2} f_5(x_t, x_h) \right. \\ \left. - \frac{19}{72} A_u^2 A_u^{*2} f_6(x_t, x_h) - \frac{19}{72} A_d A_u A_u^{*2} f_7(x_t, x_h) \right], \quad (19)$$

$$C_C^{TRR}(\mu_W) = -x_b \left[\frac{1}{16} A_u A_u^* f_3(x_t, x_h) + \frac{1}{16} A_d A_u^* f_4(x_t, x_h) + \frac{7}{96} A_d^2 A_u^{*2} f_5(x_t, x_h) \right. \\ \left. + \frac{7}{96} A_u^2 A_u^{*2} f_6(x_t, x_h) + \frac{7}{96} A_d A_u A_u^{*2} f_7(x_t, x_h) \right]. \quad (20)$$

It is noted that the Wilson coefficient $C_C^{TRR}(\mu_W)$ is now nonzero in the type-C model. To check the gauge independence of our results, we have performed the calculation both in the

Feynman and in the unitary gauge. For C^{VLL} , our results agree with the ones presented in Refs. [23,29,31]³. For C^{SRR} and C^{TRR} , on the other hand, in order to get a gauge-independent result, the external momenta of the heavy quarks inside the mesons should be taken into account, and the heavy-quark masses should be kept up to the second order; our results for these two coefficients differ from the ones presented in Refs. [23,29,31].

The QCD renormalization group (RG) evolution of these Wilson coefficients from the matching scale μ_W down to the lower scale μ_b has been calculated in Ref. [24]. One can then obtain the corresponding Wilson coefficients at the scale μ_b through [24]

$$C^{VLL}(\mu_b) = [\eta(\mu_b)]_{VLL} C^{VLL}(\mu_W), \quad (21)$$

$$\begin{pmatrix} C^{SRR}(\mu_b) \\ C^{TRR}(\mu_b) \end{pmatrix} = \begin{pmatrix} [\eta_{11}(\mu_b)]_{SRR} & [\eta_{12}(\mu_b)]_{SRR} \\ [\eta_{21}(\mu_b)]_{SRR} & [\eta_{22}(\mu_b)]_{SRR} \end{pmatrix} \begin{pmatrix} C^{SRR}(\mu_W) \\ C^{TRR}(\mu_W) \end{pmatrix}, \quad (22)$$

where the explicit expressions of the evolution factors η could be found in Ref. [24].

Equipped with the above information, the off-diagonal mass matrix element M_{12}^s is given as

$$M_{12}^s = \langle B_s^0 | \mathcal{H}_{eff}^{full} | \bar{B}_s^0 \rangle = \mathcal{A}^{VLL} + \mathcal{A}^{SRR} + \mathcal{A}^{TRR}, \quad (23)$$

where \mathcal{A}^{VLL} , \mathcal{A}^{SRR} and \mathcal{A}^{TRR} denote the contributions induced by the three four-quark operators defined by Eq. (9), respectively. Within the SM, the off-diagonal decay matrix element Γ_{12}^s can be written as [28,33]

$$\Gamma_{12}^s(SM) = - \left[\lambda_t^2 \Gamma_{12}^{cc} + 2 \lambda_t \lambda_u (\Gamma_{12}^{cc} - \Gamma_{12}^{uc}) + \lambda_u^2 (\Gamma_{12}^{cc} - 2\Gamma_{12}^{uc} + \Gamma_{12}^{uu}) \right], \quad (24)$$

with the CKM factors $\lambda_i = V_{ib}V_{is}^*$ for $i = u, c, t$. The explicit expressions for $\Gamma_{12}^{cc,uu,uc}$ could be found in Refs. [28,33]. It should be noted that Γ_{12}^s is dominated by the CKM-favored tree-level $b \rightarrow c\bar{c}s$ transition within the SM, and the NP effects are generally negligible [28]. Hence $\Gamma_{12}^s = \Gamma_{12}^s(SM)$ holds as a good approximation, which will be assumed throughout this paper.

3 Numerical results and discussions

We now proceed to present our numerical results and discussions. Values of the relevant input parameters used throughout this paper are summarized in Table 1. Our SM predictions for the

³There are two typos in Eq. (26) of Ref. [31]: a global factor 2 should be added to the term proportional to $|\eta_U|^2$ and 1/2 to the term proportional to $|\eta_U|^4$.

Table 1: Values of the relevant input parameters throughout this paper.

$ V_{us} = 0.2253 \pm 0.0008$, $ V_{ub} = 0.00413 \pm 0.00049$, $ V_{cb} = 0.0411 \pm 0.0013$, $\gamma = (68.0^{+8.0}_{-8.5})^\circ$ [34]
$\bar{m}_s(2 \text{ GeV}) = 95 \pm 5 \text{ MeV}$, $\bar{m}_b(\bar{m}_b) = 4.18 \pm 0.03 \text{ GeV}$, $m_t = 173.21 \pm 0.87 \text{ GeV}$ [34]
$\frac{\bar{m}_s(\mu)}{\bar{m}_{u,d}(\mu)} = 27.5 \pm 1.0$ [34], $m_b^{\text{pow}} = 4.8^{+0.0}_{-0.2} \text{ GeV}$ [28]
$f_{B_s} = 228 \pm 5 \pm 6 \text{ MeV}$, $f_{B_s} \sqrt{B_1} = 211 \pm 5 \pm 6 \text{ MeV}$, $f_{B_s} \sqrt{B_2} = 195 \pm 5 \pm 5 \text{ MeV}$,
$f_{B_s} \sqrt{B_3} = 215 \pm 14 \pm 9 \text{ MeV}$ [25]

Table 2: Numerical results for $\Delta M_s[\text{ps}^{-1}]$, $\Delta \Gamma_s[\text{ps}^{-1}]$, $\phi_s^{c\bar{c}s}$ and $a_{sl}^s[\%]$ within the SM. The theoretical uncertainties are obtained by varying each input parameter listed in Table 1 within its respective allowed range and then adding the individual uncertainty in quadrature.

	ΔM_s	$\phi_s^{c\bar{c}s}$	$\Delta \Gamma_s$	$a_{sl}^s[\%]$
Exp.	17.757 ± 0.021	-0.015 ± 0.035	0.081 ± 0.006	-0.75 ± 0.41
SM	$17.228^{+1.731}_{-1.672}$	$-0.043^{+0.006}_{-0.006}$	$0.082^{+0.009}_{-0.013}$	$0.0026^{+0.0004}_{-0.0004}$

observables of $B_s^0 - \bar{B}_s^0$ mixing are given in the third row of Table 2, in which the experimental data averaged by the HFAG [17] are also listed in the second row for comparison. As mentioned already in the introduction section, there is no significant deviation between the SM predictions and the experimental data for the observables at the current level of precision, even though a bit disagreement appears for a_{sl}^s . Therefore, these observables are expected to put strong constraints on the parameter spaces of 2HDMs with MFV.

From the analytic expressions of the charged-Higgs contributions to the $B_s^0 - \bar{B}_s^0$ mixing calculated in section 2.2, one can find that the model parameters relevant to our study include the two Yukawa coupling parameters A_u and A_d , as well as the charged-Higgs mass m_{H^\pm} . For the case of complex couplings, one could equivalently choose $|A_u|$ and $A_d A_u^* = |A_d A_u^*| e^{-i\theta}$ as the independent parameters, with θ being the relative phase between the two Yukawa coupling parameters. For the parameter $|A_u|$, as detailed in Ref. [14], an upper bound can be obtained from the $Z \rightarrow b\bar{b}$ decay. The parameter A_d is, however, much less constrained phenomenologically [14, 16]. Concerning the charged-Higgs mass, we shall use the LEP lower bound $m_{H^\pm}^\pm > 78.6 \text{ GeV}$ (95% CL) [35], which is obtained under the assumption that H^\pm decays dom-

inantly into fermions and does not refer to any specific Yukawa structure. Direct searches for charged-Higgs bosons are also performed by the Tevatron [36], ATLAS [37] and CMS [38] collaborations. However, most of the limits on m_H^\pm depend strongly on the assumed Yukawa structure. In this paper, we shall generate randomly numerical points for the model parameters in the ranges

$$|A_u| \in [0, 3], \quad m_H^\pm \in [80, 500] \text{ GeV}, \quad (25)$$

whereas no severe constraints for $|A_d A_u^*|$ (or $|A_d|$) and θ .

To compare the relative strength of the charged-Higgs contributions with respect to the SM one at the scale $\mu_b = m_b$, choosing $m_{H^\pm} = 200$ GeV and the default values of the input parameters listed in Table 1, we get

$$\frac{\mathcal{A}^{VLL}}{(V_{tb}V_{ts}^*)^2} \times 10^8 \simeq 3.73 + 2.00|A_u|^2 + 0.45|A_u|^4, \quad (26)$$

$$\frac{\mathcal{A}^{SRR}}{(V_{tb}V_{ts}^*)^2} \times 10^{12} \simeq -3.21|A_u|^2 + 0.69|A_u|^4 + 5.99A_d A_u^* - 3.44|A_u|^2 A_d A_u^* + 3.44A_d^2 A_u^{*2}, \quad (27)$$

$$\frac{\mathcal{A}^{TRR}}{(V_{tb}V_{ts}^*)^2} \times 10^{12} \simeq 0.03|A_u|^2 - 0.01|A_u|^4 - 0.05A_d A_u^* + 0.03|A_u|^2 A_d A_u^* - 0.03A_d^2 A_u^{*2}, \quad (28)$$

in the case of type-III model, and

$$\frac{\mathcal{A}^{VLL}}{(V_{tb}V_{ts}^*)^2} \times 10^8 \simeq 3.73 + 0.67|A_u|^2 + 0.28|A_u|^4, \quad (29)$$

$$\frac{\mathcal{A}^{SRR}}{(V_{tb}V_{ts}^*)^2} \times 10^{12} \simeq 1.10|A_u|^2 - 0.12|A_u|^4 - 2.05A_d A_u^* + 0.61|A_u|^2 A_d A_u^* - 0.61A_d^2 A_u^{*2}, \quad (30)$$

$$\frac{\mathcal{A}^{TRR}}{(V_{tb}V_{ts}^*)^2} \times 10^{12} \simeq -0.15|A_u|^2 + 0.04|A_u|^4 + 0.28A_d A_u^* - 0.18|A_u|^2 A_d A_u^* + 0.18A_d^2 A_u^{*2}, \quad (31)$$

in the case of type-C model, respectively. The number 3.73 in Eqs. (26) and (29) is the SM contribution, while the SM contributions to \mathcal{A}^{SRR} and \mathcal{A}^{TRR} are suppressed by the factor x_b , making them numerically smaller by about three orders than \mathcal{A}_{SM}^{VLL} and hence negligible. From the above numerical results, we make the following observations:

- (i) In both the type-III and type-C models, the charged-Higgs contributions to \mathcal{A}^{VLL} (Eqs. (26) and (29)) depend only on the Yukawa coupling parameter A_u via $|A_u|$, and hence are always constructive to the SM one. For a value $|A_u| \sim \mathcal{O}(1)$, the type-III contribution

could be comparable with the SM one, while the type-C model provides a relatively smaller correction.

- (ii) Comparing Eqs. (27)-(28) with (26) (for the type-III model) and Eqs. (30)-(31) with (29) (for the type-C model), one can see that the NP contributions to \mathcal{A}^{SRR} and \mathcal{A}^{TRR} are much smaller than to \mathcal{A}^{VLL} , especially when $|A_d| \sim |A_u|$. This is because the Wilson coefficients $C^{SRR}(\mu_W)$ and $C^{TRR}(\mu_W)$ are always suppressed by the factor x_b with respect to $C^{VLL}(\mu_W)$, both within the SM and in the 2HDMs with MFV.
- (iii) In the case with large complex values of $A_d A_u^*$, however, the charged-Higgs contributions to \mathcal{A}^{SRR} and \mathcal{A}^{TRR} could provide a large imaginary part to the off-diagonal mass matrix element M_{12}^s , which may result in a significant correction to the CP-violating observables, such as ϕ_s and $\phi_s^{c\bar{c}s}$.
- (iv) Different from the type-C model, the type-III contribution to \mathcal{A}^{TRR} is induced only by the RG evolution effect, and is numerically much smaller. There are, however, cancelations between the charged-Higgs contributions to \mathcal{A}^{SRR} and \mathcal{A}^{TRR} in the type-C model.

It is therefore expected that the current experimental data on $B_s^0 - \bar{B}_s^0$ mixing could put some constraints on the model parameters and be used to distinguish between these two models.

To get the explicitly allowed parameter spaces, we perform the analysis with the following procedure: we scan the parameter spaces within the ranges specified by Eq. (25), with the value of m_{H^\pm} fixed at 100, 250 and 500 GeV, respectively. At each point in the parameter spaces, we evaluate the theoretical prediction for an observable, together with the corresponding theoretical uncertainty induced by the input parameters listed in Table 1. The theoretical range for an observable at each point is obtained by varying each input parameter within its respective allowed range and then adding the individual uncertainty in quadrature. If the obtained theoretical range has overlap with the 2σ range of the experimental data, the point is regarded as allowed. In addition, we consider two different cases: real and complex couplings with respect to A_u and A_d . Under the combined constraints from ΔM_s , $\phi_s^{c\bar{c}s}$ and a_{sl}^s , the allowed parameter spaces of the type-III and type-C models are shown in Figs. 2 (for the case of real couplings) and 3 (for the case of complex couplings), respectively.

For the case of real couplings, it can be seen from Fig. 2 that:

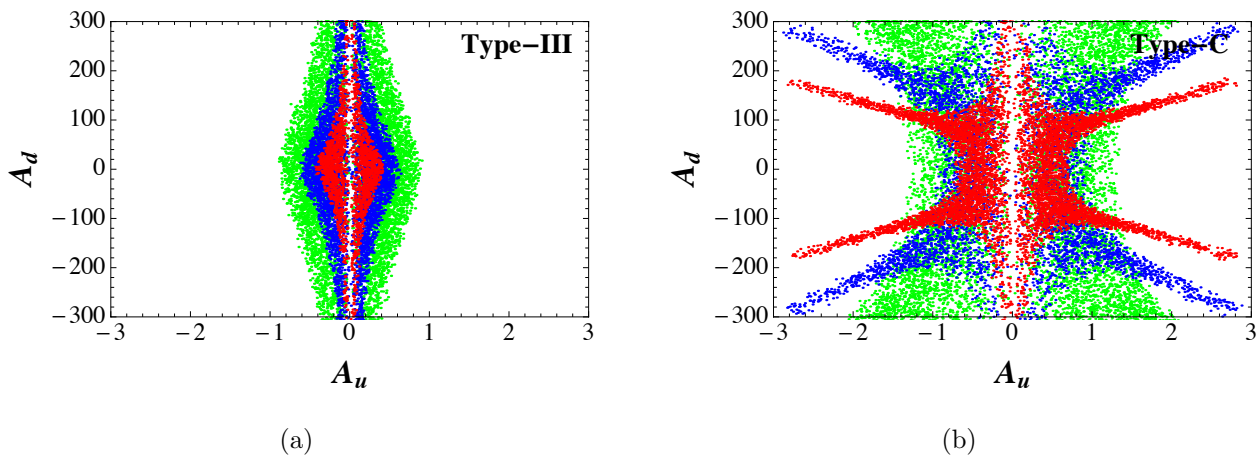


Figure 2: Allowed spaces of the parameters A_u and A_d in type-III and type-C models under the combined constraints from ΔM_s , $\phi_s^{c\bar{c}s}$ and a_{sl}^s , in the case of real couplings. The red, blue and green pointed regions are obtained with $m_{H^\pm} = 100, 250$ and 500 GeV, respectively.

- (i) In the type-III model, as shown in Fig. 2(a), the module of Yukawa coupling parameter A_u is severely constrained by the good agreement between the SM prediction and the experimental data for ΔM_s ; for instance $|A_u| < 1$ is obtained with $m_{H^\pm} = 500$ GeV. There are, however, almost no constraints on the coupling A_d , because the contribution involving it is negligible with respect to the one involving only A_u .
- (ii) In the type-C model, because the charged-Higgs contribution to \mathcal{A}^{VLL} is relatively small and large cancelation effects exist between the terms involving A_d and A_u , the allowed values of A_d and A_u could be large simultaneously, with either the same or the opposite signs, as shown by the four “legs” in Fig. 2(b).
- (iii) Besides the “legs” in Fig. 2(b), the difference between the two models is also featured by the different shapes of the allowed parameter spaces. The current data on $B_s^0 - \bar{B}_s^0$ mixing generally puts a stronger constraint on the type-III model; for instance, with the assumption $|A_d| \sim |A_u|$ and choosing $m_{H^\pm} = 500$ GeV, the upper bound $|A_u| \sim 1.5$ obtained in type-C model is obviously looser than the one $|A_u| \sim 1$ in type-III model.

For the case of complex couplings, one more model parameter θ is introduced. From Fig. 3, it is found that:

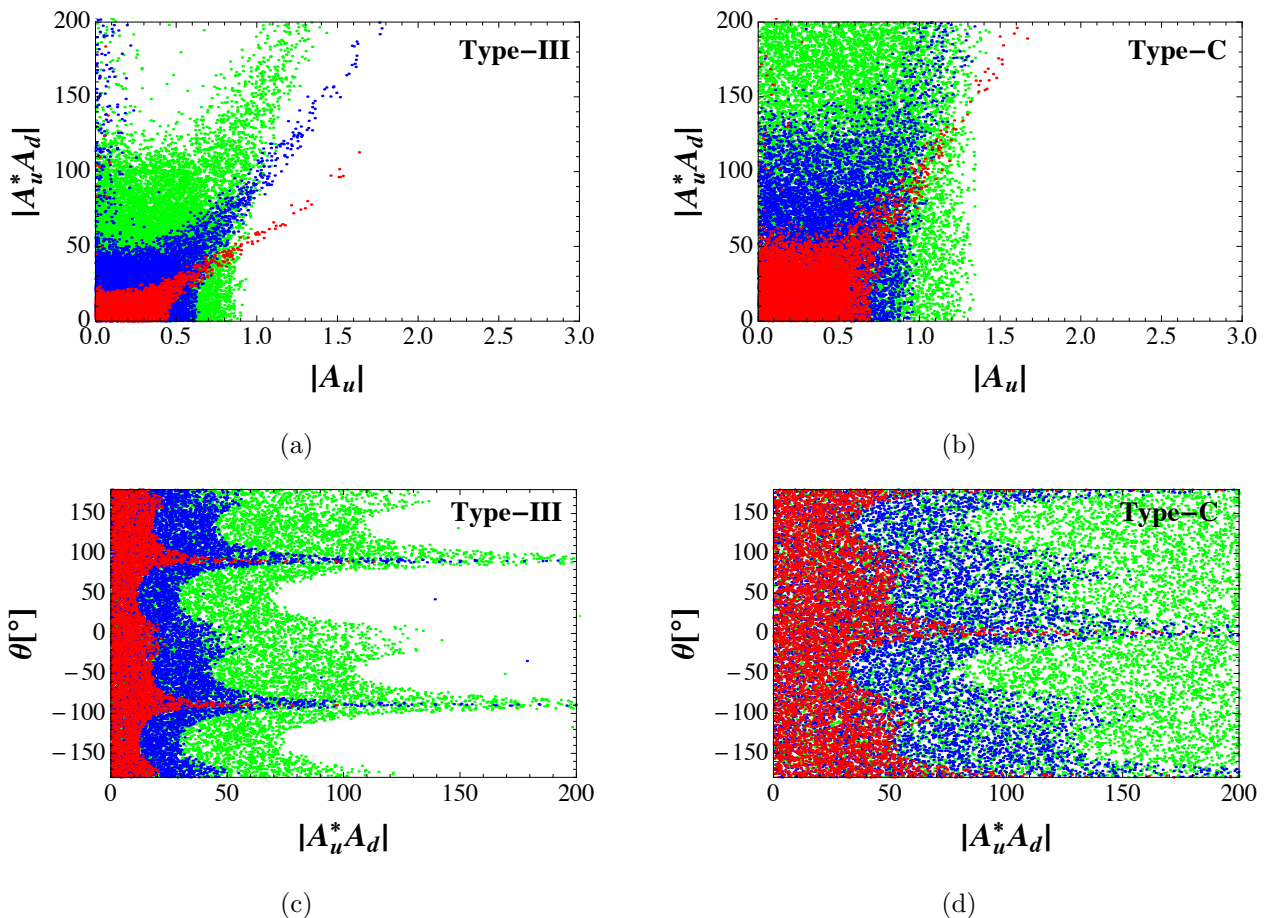


Figure 3: Allowed spaces of the parameters $|A_u|$, $|A_u^* A_d|$ and θ in type-III and type-C models under the combined constraints from ΔM_s , $\phi_s^{c\bar{c}s}$ and a_{sl}^s , in the case of complex couplings. The other captions are the same as in Fig. 2.

- (i) In the type-III model, as shown in Figs. 3(a) and 3(c), large values of $|A_u|$ and $|A_u^* A_d|$ are still allowed around $\theta \sim \pm 90^\circ$, which makes it different from the case of real couplings. This is due to the fact that large cancellation effects appear among the charged-Higgs contributions when $\theta \sim \pm 90^\circ$, which can also be seen from Eqs. (27) and (28). Moreover, as shown in Fig. 3(a), an approximately linear relationship is observed between $|A_u^* A_d|$ and $|A_u|$ when $|A_u| \gtrsim 0.5$.
- (ii) As shown in Figs. 3(b) and 3(d), similar observations could also be made in the type-C model, except for the fact that the constraints on the model parameters are now much looser. In addition, the cancellation effects among the charged-Higgs contributions occur

around $\theta \sim 0^\circ$ and $\pm 180^\circ$, which is different from that observed in the type-III model.

From the above discussions, we conclude that the type-III and type-C models exhibit some significantly different behaviors under the experimental constraints from $B_s^0 - \bar{B}_s^0$ mixing. However, due to the large theoretical and experimental uncertainties, the differences in the small $|A_u|$ and $|A_d|$ ranges are hardly to be distinguished from each other. The future refined measurement and precise theoretical evaluation for $B_s^0 - \bar{B}_s^0$ mixing might show a much clearer phenomenological picture for the type-III and type-C models.

As a final comment, it should be noted that the same analysis could also be applied to the $B_d^0 - \bar{B}_d^0$ mixing, which is another important related low-energy process. The charged-Higgs effect on it can be obtained from that on the $B_s^0 - \bar{B}_s^0$ mixing, with the replacement $s \rightarrow d$ throughout the theoretical formulae presented in Sec. 2.2. However, we find that the bounds on the model parameters derive from the $B_d^0 - \bar{B}_d^0$ mixing are quite similar to the ones from the $B_s^0 - \bar{B}_s^0$ mixing, and no any further information on the model parameters could be obtained from the former. Therefore, the constraints from $B_d^0 - \bar{B}_d^0$ mixing will not be shown here.

4 Conclusion

In this paper, we have calculated the one-loop electro-weak corrections to the $B_s^0 - \bar{B}_s^0$ mixing within the type-III and type-C 2HDMs with MFV, in which the second scalar doublet is fixed to be color-singlet and color-octet, respectively. It is noted that, in order to get a gauge-independent result, the external momenta of the heavy quarks inside the mesons should be taken into account, and the heavy-quark masses should be kept up to the second order.

Based on the obtained short-distance Wilson coefficients of the four-quark operators appearing in the effective weak Hamiltonian, and combining the up-to-date experimental data on $B_s^0 - \bar{B}_s^0$ mixing, we then performed a detailed phenomenological analysis of the charged-Higgs effects on this process. Our main conclusions are summarized as follows:

- (i) While the type-C model gives a nonzero contribution to the Wilson coefficient $C_C^{TRR}(\mu_W)$, the type-III contribution to the amplitude \mathcal{A}^{TRR} is induced only by RG evolution effect.
- (ii) In the case of real couplings, the allowed spaces of the Yukawa coupling parameters A_u and A_d in the two models are obviously different, as shown in Fig. 2.

- (iii) In the case of complex couplings, due to the cancelation effects among the charged-Higgs contributions, large values of $|A_u|$ and $|A_d|$ are still allowed around $\theta \sim \pm 90^\circ$ in the type-III and around $\theta \sim 0^\circ, \pm 180^\circ$ in the type-C model, which is shown in Fig. 3.

The observed differences could be used to distinguish the two models. It should be noted, however, that their differences in the small $|A_d|$ and $|A_u|$ ranges are hardly to be distinguished, due to the large theoretical and experimental uncertainties. More refined theoretical and experimental efforts are therefore needed for a much clearer phenomenological picture.

Acknowledgments

We thank Antonio Pich and Martin Jung for useful discussions and cross-checks for the box Feynman diagrams. This work is supported by the National Natural Science Foundation of China (Grant Nos. 11475055, 11435003, 11105043 and 11005032). Q. Chang is also supported by the Foundation for the Author of National Excellent Doctoral Dissertation of P. R. China (Grant No. 201317) and the Program for Science and Technology Innovation Talents in Universities of Henan Province (No. 14HASTIT036). X. Q. Li is also supported by the Scientific Research Foundation for the Returned Overseas Chinese Scholars, State Education Ministry, by the Open Project Program of SKLTP, ITP, CAS, China (No. Y4KF081CJ1), and by the self-determined research funds of CCNU from the colleges' basic research and operation of MOE (CCNU15A02037).

A Relevant coefficients for $B_s^0 - \bar{B}_s^0$ mixing

Here we present the explicit expressions for $f_i(x_t, x_h)$ appearing in Eqs. (15) and (18):

$$f_1(x_t, x_h) = \frac{1}{2} \left[\frac{x_t^2(x_t - 4)}{(x_h - x_t)(1 - x_t)} + \frac{x_t^2(3x_t^2 - x_h(4 - 2x_t + x_t^2)) \ln x_t}{(x_h - x_t)^2(1 - x_t)^2} - \frac{(x_h - 4)x_h x_t^2 \ln x_h}{(1 - x_h)(x_h - x_t)^2} \right], \quad (32)$$

$$f_2(x_t, x_h) = \frac{1}{2} \left[\frac{x_t^2(x_h + x_t)}{2(x_h - x_t)^2} + \frac{x_h x_t^3 \ln x_t}{(x_h - x_t)^3} - \frac{x_h x_t^3 \ln x_h}{(x_h - x_t)^3} \right], \quad (33)$$

$$f_3(x_t, x_h) = \frac{1}{3} \left[- \frac{x_t^2(x_t^2 + x_h^4)(-11 + 7x_t - 2x_t^2) + x_h x_t^3(7 + 53x_t - 55x_t^2 + 19x_t^3)}{3(1 - x_h)^2(x_h - x_t)^3(1 - x_t)^3} \right]$$

$$\begin{aligned}
& - \frac{x_h^2 x_t^2 (-2 - 55x_t + 15x_t^2 + 17x_t^3 - 11x_t^4) + x_h^3 x_t^2 (19 + 17x_t - 19x_t^2 + 7x_t^3)}{3(1-x_h)^2(x_h-x_t)^3(1-x_t)^3} \\
& + \frac{2x_t^2(x_h^3 - 3x_h^2x_t + 3x_hx_t^2 - 3x_t^4 + 3x_t^5 - x_t^6) \ln x_t}{(x_h-x_t)^4(1-x_t)^4} \\
& - \frac{2x_hx_t^2(x_h^2 + (-3+x_h)x_hx_t + (3+(-3+x_h)x_h)x_t^2) \ln x_h}{(1-x_h)^3(x_h-x_t)^4} \Big], \tag{34}
\end{aligned}$$

$$\begin{aligned}
f_4(x_t, x_h) = & - \frac{x_t^2((x_h^2 + x_t)(-3 + x_t) + x_h(1 + 6x_t - 3x_t^2))}{2(1-x_h)(x_h-x_t)^2(1-x_t)^2} \\
& - \frac{x_t^2(x_h^2 - 2x_hx_t - (-2 + x_t)x_t^3) \ln x_t}{(x_h-x_t)^3(1-x_t)^3} + \frac{x_hx_t^2(x_h - 2x_t + x_hx_t) \ln x_h}{(1-x_h)^2(x_h-x_t)^3}, \tag{35}
\end{aligned}$$

$$f_5(x_t, x_h) = - \frac{2x_t^2}{(x_h-x_t)^2} - \frac{x_t^2(x_h+x_t) \ln x_t}{(x_h-x_t)^3} + \frac{x_t^2(x_h+x_t) \ln x_h}{(x_h-x_t)^3}, \tag{36}$$

$$\begin{aligned}
f_6(x_t, x_h) = & \frac{1}{6} \Big[- \frac{x_t^2(5x_h^2 - 22x_hx_t + 5x_t^2)}{3(x_h-x_t)^4} - \frac{x_t^2(x_h^3 - 3x_h^2x_t - 3x_hx_t^2 + x_t^3) \ln x_t}{(x_h-x_t)^5} \\
& + \frac{x_t^2(x_h^3 - 3x_h^2x_t - 3x_hx_t^2 + x_t^3) \ln x_h}{(x_h-x_t)^5} \Big], \tag{37}
\end{aligned}$$

$$f_7(x_t, x_h) = \frac{2x_t^2}{(x_h-x_t)^2} + \frac{x_t^2(x_h+x_t) \ln x_t}{(x_h-x_t)^3} - \frac{x_t^2(x_h+x_t) \ln x_h}{(x_h-x_t)^3}. \tag{38}$$

References

- [1] G. Aad *et al.* [ATLAS Collaboration], Phys. Lett. B **716** (2012) 1.
- [2] S. Chatrchyan *et al.* [CMS Collaboration], Phys. Lett. B **716** (2012) 30.
- [3] G. Aad *et al.* [ATLAS Collaboration], Phys. Lett. B **726** (2013) 88 [Erratum-ibid. B **734** (2014) 406]; Phys. Lett. B **726** (2013) 120; The ATLAS collaboration, ATLAS-CONF-2014-009; ATLAS-COM-CONF-2014-013.
- [4] S. Chatrchyan *et al.* [CMS Collaboration], Nature Phys. **10** (2014) 557; V. Khachatryan *et al.* [CMS Collaboration], arXiv:1411.3441 [hep-ex]; arXiv:1412.8662 [hep-ex].
- [5] T. Aaltonen *et al.* [CDF and D0 Collaborations], Phys. Rev. D **88** (2013) 052014; B. Tuchming [CDF and D0 Collaborations], arXiv:1405.5058 [hep-ex].
- [6] T. D. Lee, Phys. Rev. D **8** (1973) 1226.

- [7] S. L. Glashow, J. Iliopoulos and L. Maiani, Phys. Rev. D **2** (1970) 1285.
- [8] S. L. Glashow and S. Weinberg, Phys. Rev. D **15** (1977) 1958.
- [9] A. J. Buras, P. Gambino, M. Gorbahn, S. Jager and L. Silvestrini, Phys. Lett. B **500** (2001) 161; G. D'Ambrosio, G. F. Giudice, G. Isidori and A. Strumia, Nucl. Phys. B **645** (2002) 155; A. J. Buras, M. V. Carlucci, S. Gori and G. Isidori, JHEP **1010**, 009 (2010); E. Cervero and J. M. Gerard, Phys. Lett. B **712** (2012) 255.
- [10] A. M. Hadeed and B. Holdom, Phys. Lett. B **159** (1985) 379; G. C. Branco, W. Grimus and L. Lavoura, Phys. Lett. B **380** (1996) 119 [hep-ph/9601383]; F. J. Botella, G. C. Branco and M. N. Rebelo, Phys. Lett. B **687** (2010) 194 [arXiv:0911.1753 [hep-ph]]; F. J. Botella, G. C. Branco, A. Carmona, M. Nebot, L. Pedro and M. N. Rebelo, JHEP **1407** (2014) 078 [arXiv:1401.6147 [hep-ph]]; G. Bhattacharyya, D. Das and A. Kundu, Phys. Rev. D **89** (2014) 095029 [arXiv:1402.0364 [hep-ph]].
- [11] G. C. Branco, P. M. Ferreira, L. Lavoura, M. N. Rebelo, M. Sher and J. P. Silva, Phys. Rept. **516** (2012) 1; J. F. Gunion, H. E. Haber, G. L. Kane and S. Dawson, Front. Phys. **80** (2000) 1.
- [12] S. Davidson and H. E. Haber, Phys. Rev. D **72** (2005) 035004 [Erratum-ibid. D **72** (2005) 099902].
- [13] A. V. Manohar and M. B. Wise, Phys. Rev. D **74** (2006) 035009.
- [14] G. Degrossi and P. Slavich, Phys. Rev. D **81** (2010) 075001.
- [15] A. Pich and P. Tuzon, Phys. Rev. D **80** (2009) 091702.
- [16] X. Q. Li, Y. D. Yang and X. B. Yuan, Phys. Rev. D **89** (2014) 054024.
- [17] Y. Amhis *et al.* [Heavy Flavor Averaging Group (HFAG) Collaboration], arXiv:1412.7515 [hep-ex], and online update at: <http://www.slac.stanford.edu/xorg/hfag>.
- [18] A. Lenz and U. Nierste, arXiv:1102.4274.
- [19] A. Lenz, Nucl. Phys. Proc. Suppl. **81** (2008) 177.

- [20] N. Cabibbo, Phys. Rev. Lett. **10** (1963) 531.
- [21] M. Kobayashi and T. Maskawa, Prog. Theor. Phys. **49** (1973) 652.
- [22] A. J. Buras, M. Jamin and P. H. Weisz, Nucl. Phys. B **347** (1990) 491.
- [23] J. Urban, F. Krauss, U. Jentschura and G. Soff, Nucl. Phys. B **523** (1998) 40.
- [24] A. J. Buras, S. Jager and J. Urban, Nucl. Phys. B **605** (2001) 600; A. J. Buras, M. Misiak and J. Urban, Nucl. Phys. B **586** (2000) 397.
- [25] N. Carrasco *et al.* [ETM Collaboration], JHEP **1403** (2014) 016; N. Carrasco, arXiv:1410.0161 [hep-lat].
- [26] G. Buchalla, A. J. Buras and M. E. Lautenbacher, Rev. Mod. Phys. **68** (1996) 1125; A. J. Buras, hep-ph/9806471.
- [27] T. Inami and C. S. Lim, Prog. Theor. Phys. **65** (1981) 297 [Erratum-ibid. **65** (1981) 1772].
- [28] A. Lenz and U. Nierste, JHEP **0706** (2007) 072; A. J. Lenz, Phys. Rev. D **84** (2011) 031501.
- [29] A. J. Buras, P. H. Chankowski, J. Rosiek and L. Slawianowska, Nucl. Phys. B **619** (2001) 434; Nucl. Phys. B **659** (2003) 3; G. Isidori and A. Retico, JHEP **0111** (2001) 001 [hep-ph/0110121].
- [30] M. Jung, A. Pich and P. Tuzon, JHEP **1011** (2010) 003.
- [31] A. V. Manohar and M. B. Wise, Phys. Rev. D **74** (2006) 035009 [hep-ph/0606172].
- [32] X. D. Cheng, X. Q. Li, Y. D. Yang and X. Zhang, arXiv:1504.00839 [hep-ph].
- [33] M. Beneke, G. Buchalla and I. Dunietz, Phys. Rev. D **54** (1996) 4419 [Erratum-ibid. D **83** (2011) 119902]; M. Beneke, G. Buchalla, C. Greub, A. Lenz and U. Nierste, Phys. Lett. B **459** (1999) 631; M. Beneke, G. Buchalla, A. Lenz and U. Nierste, Phys. Lett. B **576** (2003) 173.

- [34] K. A. Olive *et al.* [Particle Data Group Collaboration], *Chin. Phys. C* **38** (2014) 090001.
- [35] G. Abbiendi *et al.* [ALEPH and DELPHI and L3 and OPAL and LEP Collaborations], *Eur. Phys. J. C* **73** (2013) 2463.
- [36] P. Gutierrez [CDF and D0 Collaborations], *PoS CHARGED* **2010** (2010) 004.
- [37] G. Aad *et al.* [ATLAS Collaboration], *Eur. Phys. J. C* **73** (2013) 6, 2465; *JHEP* **1503** (2015) 088; arXiv:1503.04233 [hep-ex].
- [38] CMS Collaboration [CMS Collaboration], CMS-PAS-HIG-13-035; CMS-PAS-HIG-14-020.